Molecular Crystals and Liquid Crystals
Publication details, including instructions for authors and subscription information:
http://www.tandfonline.com/loi/gmcl16

Inducing Cholesteric-Texture Changes by Means of Two-Frequency Addressable Liquid Crystal Material

Paul R. Gerber [a]
[a] Centeral Research Units, F. Hoffmann-La Roche & Co. Ltd., Basel, Switzerland, CH-4002
Version of record first published: 17 Oct 2011.

To cite this article: Paul R. Gerber (1985): Inducing Cholesteric-Texture Changes by Means of Two-Frequency Addressable Liquid Crystal Material, Molecular Crystals and Liquid Crystals, 124:1, 163-177

To link to this article: http://dx.doi.org/10.1080/00268948508079474

Mol. Cryst. Liq. Cryst., 1985, Vol. 124, pp. 163–177
0026-8941/85/1244–163/$20.00/0

Printed in the United States of America

Inducing Cholesteric-Texture Changes by Means of Two-Frequency Addressable Liquid Crystal Material†

PAUL R. GERBER

Central Research Units, F. Hoffmann-La Roche & Co. Ltd., CH-4002 Basel/Switzerland

(*Received July 26, 1984*)

Cholesteric material of suitable pitch can show brillant reflection colours if arranged in a planar Grandjean state. In the fingerprint state forward scattering prevails. With a light-absorbing background these two states provide the basis for a display with storage properties. Two-frequency addressable materials provide a convenient way of switching between the two states. In addition they allow the generation of dynamic scattering in a limited frequency range. In the present work the textures are studied by means of light reflection. It is shown that the dynamic scattering mechanism leads to different characteristic textures as compared to switching by electric torques alone. Furthermore, the angular distribution of reflected light in the Grandjean state is studied for various preparation conditions. It is found that roughly half of the reflected light leaves under non-specular angles on average with a deviation of about 25 degrees. Driving conditions for a working multiplexed matrix display are given.

1. INTRODUCTION

In thin layers cholesteric materials can show various textures,[1] the most prominent of which are the Grandjean (or planar) texture in which the cholesteric helix axis lies perpendicular to the substrates, and the fingerprint texture with the helix axis in the substrate plane. The periodicity of the cholesteric structure leads to the possibility of

†Paper presented at the 10th International Liquid Crystal Conference, York, 15th–21st July 1984.

reflection of light if its wavelength in the cholesteric medium, λ_{chol}, obeys the Bragg-reflection condition[1]

$$\lambda_{chol} = \mathbf{p} \cdot \cos\theta, \tag{1.1}$$

where $\mathbf{p}$ is the cholesteric pitch and θ the angle of propagation with respect to the cholesteric helix axis. In the Grandjean state (1.1) implies back reflection of suitably polarized light,[1] while in the fingerprint texture reflection takes place in forward direction such that all light passes through the cell. Before an absorbing background the two states thus provide the basis for a reflective display device,[2] provided the two states can be generated by suitable means. Switching in one direction is easily achieved by the orienting forces of an electrical field, while backswitching processes include mechanical shearing, thermal treatment and the generation of electrohydrodynamic turbulence. Recently the use of a two-frequency addressable material was shown to provide a relatively convenient way of switching between the two states,[3] because orienting torques of either sign can be generated. In addition, at suitable frequencies the condition for the occurrence of electrohydrodynamic instabilities is fulfilled,[4] thus providing an additional switching mechanism.

It is the purpose of this work to study some properties of the various Grandjean and fingerprint like states which may well depend on the switching mechanism. In addition, the influence of various parameters on driving conditions in a display application is examined in order to provide a basis for optimization of this application.

2. MATERIALS

The basic mixture is a commercial two-frequency addressable mixture (3090 from F. Hoffmann-La Roche)[5] with the following properties:

Clearing temperature	$T_c = 81°C$
Indices of refraction	$n_\parallel = 1.60$
	$n_\perp = 1.50$
Dielectric constants	$\epsilon_\perp = 9.56$
	$\epsilon_\parallel(f = 40\ \text{Hz}) = 15.25$
	$\epsilon_\parallel(f = 10\ \text{kHz}) = 4.85$
Crossover frequency	$f_c(\epsilon_\parallel = \epsilon_\perp) = 420\ \text{Hz}$
Bulk viscosity	$\eta = 1.09$ Poise
Rotational viscosity	$\gamma_1 = 5.4$ Poise

Elastic constants $k_{11} = 11.8 \cdot 10^{-12}$N
$k_{22}/k_{11} = 0.47$
$k_{33}/k_{11} = 1.06$

at room temperature (22°C).

An interesting aspect of dual frequency materials is that they enable the generation of electrohydrodynamic instabilities without the presence of ionic components. In a suitable frequency range the relaxation process of the long polar molecules in the mixture, which leads to the dispersion behaviour of the dielectric constant, provides the Ohmic conductivity which is required for the dynamic scattering process.[6] Figure 1 shows the region of occurrence of hydrodynamic instabilities in the frequency-voltage plane for the mixture 3090. Observations were made in a 10 μm-spaced cell with homogeneous in-plane alignment conditions induced by oblique evaporation of SiO on both glass substrates. Also shown is the wave number of the distortion pattern as observed upon raising the voltage at a given frequency just across the threshold value.

In order to obtain a cholesteric material chiral molecules must be added. These have to fulfill quite stringent requirements such as:

1) high helical twisting power to induce small-pitch cholesteric properties at low concentrations,
2) little depressing influence on the clearing temperature,
3) high solubility to yield the required pitch with as few components as possible, and
4) small axial electric dipole moment in order not to spoil the negative high-frequency dielectric anisotropy.

The diester[7]

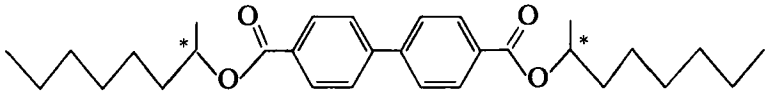

(I)

obeys most of these requirements, except for point 2. To obtain a right handed cholesteric material reflecting in the yellow-green about 13% w/w of (I) was added to mixture 3090. The resulting pitch is shown in Figure 2 as a function of temperature. Unfortunately the clearing temperature of this mixture was 38°C degrees below that of pure 3090 and the two-phase region (cholesteric-isotropic) increased from 15°C to roughly 30°C. Due to this drop in T_c and the accompanying decrease in the order parameter the crossover frequency f_c increased by almost an order of magnitude (Figure 2). The strong

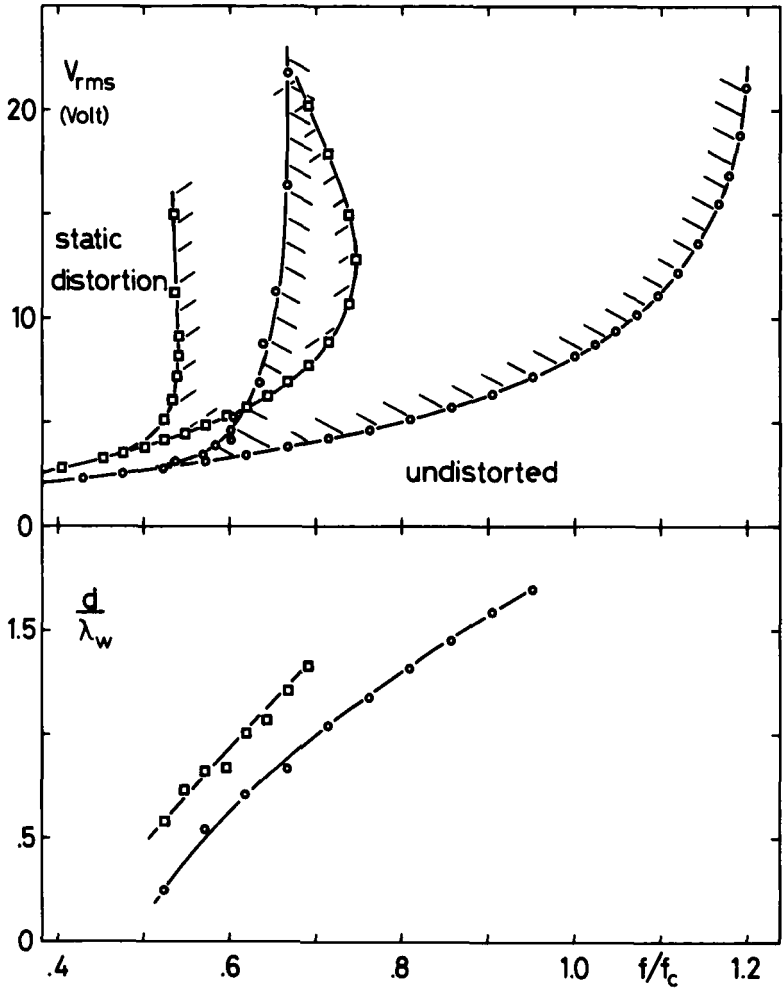

FIGURE 1 Domains of occurrence of electrohydrodynamic instabilities in the frequency voltage plane for sinusoidal (circles) and square wave (squares) applied voltages. Also shown is the ratio of cell spacing d (10 μm) to wavelength λ_w of Williams stripes at the onset of the stability as a function of frequency. These graphs end at an upper limiting frequency where the instability sets in in a non stationary mode. The scale of the abseissa is in error. To obtain the correct values, multiply by $\pi/2$.

temperature dependence of f_c observed in 3090 is also seen in the mixture with I. For the reflection measurements of the next section, an additional 11% w/w mixture was prepared in order to generate Bragg reflections for red light.

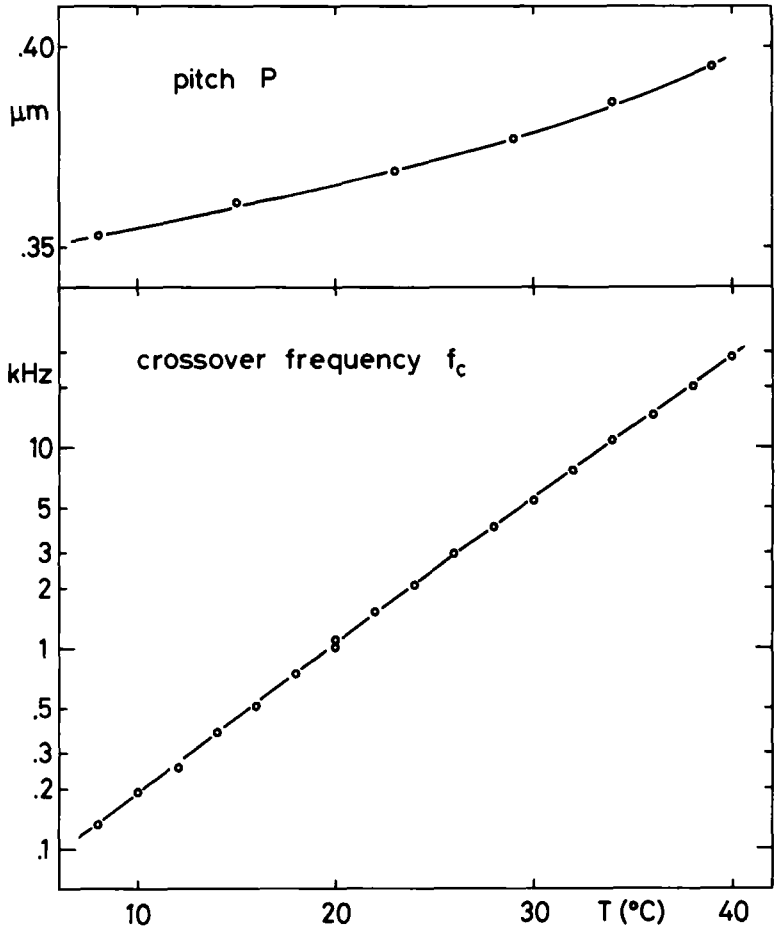

FIGURE 2 Pitch **p** and crossover frequency f_c as a function of temperature for the mixture of 13% by weight of (I) added to 3090. The crossover frequency was determined indirectly by applying a 50 rms square wave voltage to a 10 μm-spaced sandwich cell. Upon lowering the frequency the onset of a hydrodynamic instability was observed. The frequency of this onset was taken as f_c which may not be entirely correct but adequate for the purpose of applications.

3. REFLECTION OF LIGHT

The experiments of this section were performed with a 10 μm spaced cell, the glass substrates of which were treated by oblique evaporation of SiO to induce homogeneous in-plane alignment of the director at the surface. To enable straight-forward experimentation with a

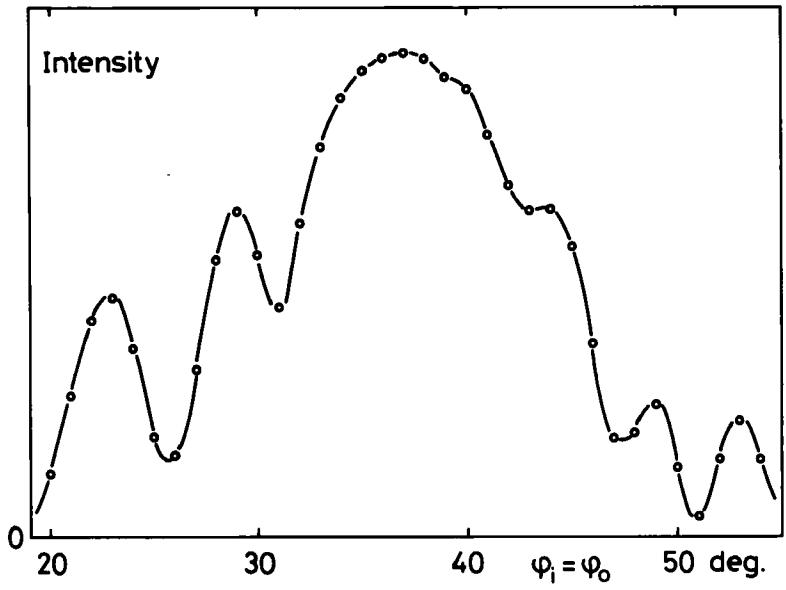

FIGURE 3 Intensity of light (in arbitrary units) reflected at specular conditions from a cholesteric layer in the Grandjean state generated by cycle 1 (section 3.2) as a function of the angle of incidence ϕ_i.

He-Ne laser of wavelength $\lambda_0 = 0.632$ nm, the 11% mixture (section 2) which showed a pitch of $\mathbf{p} = 0.44$ μm was used.

3.1 Geometry

Laser light was directed on the cell with the plane of incidence coinciding with the plane defined by the substrate normal and the direction of alignment of the nematic director at the substrate. Reflected light was observed in the same plane. The angles of incidence and observation are called ϕ_i and ϕ_0 respectively, where $\phi_i = \phi_0$ defines specular reflection from the substrate plane. Two types of experiments were performed. The first kept specular conditions $\phi_i = \phi_0$ with both angles varying simultaneously by the same amount. For the second type the sum $\phi_i + \phi_0 = 2\alpha$ was kept fixed and the cell was rotated by an angle ϕ away from specular conditions. With increasing ϕ the cell normal turns towards the laser ($\phi_i = \alpha - \phi$, $\phi_0 = \alpha + \phi$). The polarization direction of the laser was chosen such as to maximize the specular reflection of the Grandjean state at an angle $\phi_i = \phi_0 = 37°$ which corresponds to the center of the Bragg

reflection band. This maximum occurred by turning the plane of polarization away from the plane of incidence by 58° such that turning sense and direction of light propagation resulted in a left-handed screw-sense.

Clearly, the chosen geometry is only a very restricted fraction of the full set of parameter values needed to fully characterize the system. Nevertheless, we hope that the present measurements reveal some of the features which are of importance for application in a reflective display.

3.2 Switching cycles

The textures considered in this work are only approximately described by the ideal Grandjean or fingerprint structures. In fact they all contain a net of disclinations which is subject to hysteresis effects. Thus the properties of what we call the Grandjean state depend, to some extent, on the history of past switching processes and on aging. In order to prepare relatively well defined states we pretreated the cell by running either of the two following cycles several times.

Cycle 1: −30 sec. application of a low frequency (400 Hz) 60 V_{rms} square wave −30 sec. without an applied voltage −30 sec. application of a high frequency (12 kHz) 60 V_{rms} square wave −30 sec. without an applied voltage.

Cycle 2: As cycle 1 but instead of a low frequency (400 Hz) a voltage medium frequency (1.5 kHz) was chosen which led to the generation of dynamic scattering. The 30 sec. time intervals proved to be sufficient to achieve steady state conditions in each case.

The two cycles were chosen in order to find possible differences in the two mechanisms—dynamic scattering and electrostatic reorientation—of generating a fingerprint-like state.

3.3 General features of light reflection

Figure 3 shows the intensity of the laser light reflected from the liquid crystal layer in a Grandjean texture of cycle 1, under specular geometry ($\phi_i = \phi_0$), as a function of the angle ϕ_i. A broad maximum is seen with a superimposed interference pattern which originates from the partially reflecting SnO_2 electrode layers and which we will neglect here. The width of the maximum is well explained by the width of the Bragg reflection band when transformed from wavelength dependence to angular dependence for monochromatic light through equation (1.1). Thus, the range of angles showing Bragg

reflection is given by

$$\arcsin(n_\perp^2 - (\lambda_0/\mathbf{p})^2)^{1/2} < \phi_i < \arcsin(n_\parallel^2 - (\lambda_0/\mathbf{p})^2)^{1/2} \quad (3.1)$$

From Figure 3 a value of $\phi_{i,\max} = 37°$ is deduced for the center of the reflection band.

With this information we performed the following measurements aimed at characterizing the texture under consideration. The cell was rotated with the sum of angles $\phi_i + \phi_0 = 2\alpha = 2\phi_{i,\max}$ held constant as described in section 3.1. Figure 4 shows a typical plot of intensity versus cell rotation angle ϕ as obtained from a Grandjean state of cycle 1. An intense central peak is surrounded by a halo of diffusely scattered light. The distribution of the diffusely scattered intensity is non-symmetric with respect to replacing ϕ by $-\phi$. This may be caused by the varying degree of ellipticity of the light after it has entered the sample. Characteristic features are the strong oscillations in intensity with varying ϕ and the two pronounced maxima around $\phi = \pm 9$ degrees.

The oscillations may be explained, somewhat heuristically, by the presence of a large number of cholesteric domains with slightly tilted

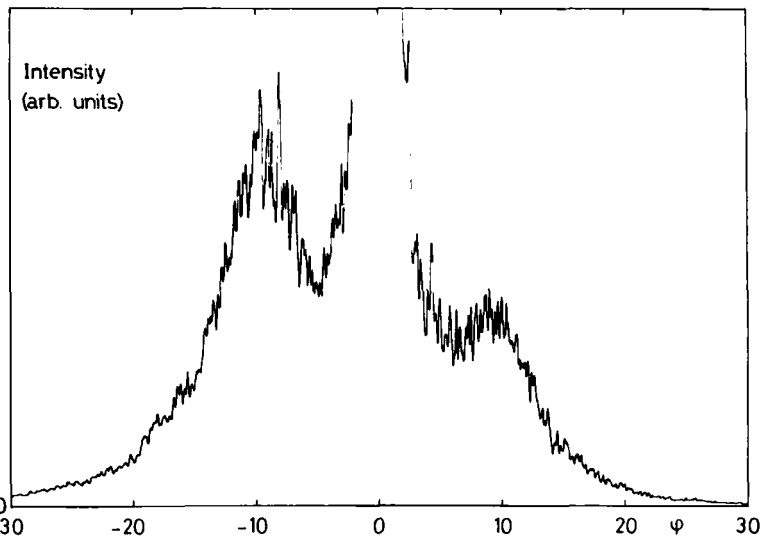

FIGURE 4 Typical plot of reflected intensity versus turning angle of cell away from specular conditions. Laser and detector are kept at fixed positions. The central feature is out of scale by several orders. The cholesteric layer was in the Grandjean state of cycle 1.

helix axes relative to the substrate normal. The sharp peaks in the noisy intensity plot would, thus, correspond to single domains oriented exactly under specular conditions. With this interpretation the distribution in Figure 4 may be translated into a distribution of helix-axis directions of cholesteric domains. For a given angle ϕ one can, thus, approximately determine the angle χ between the substrate normal and the helix-axis of the domains under specular conditions through:

$$\chi \approx \frac{1}{2}\left[\arcsin\left(\frac{\sin(\alpha + \phi)}{\bar{n}}\right) - \arcsin\left(\frac{\sin(\alpha - \phi)}{\bar{n}}\right)\right]. \quad (3.2)$$

Both contributions, the specular peak intensity and the diffusely reflected light, will prove useful in characterizing and distinguishing between various cholesteric textures.

3.4 Limiting textures of cycles 1 and 2

When measuring the intensity of the specularly reflected light, when running the cycles 1 and 2, pronounced differences between the two cycles can be observed as shown in Figure 5. With the high frequency voltage applied the limiting texture of cycle 1 develops a considerably higher limiting intensity than that of cycle 2. This difference is, however, reduced upon removing the voltage.

With the low (or medium for cycle 2) frequency voltage applied it takes considerably more time to reach a stationary reflection in cycle 2 than in cycle 1. Upon removing the voltage, a fairly large amount of intensity recovers in cycle 2, in contrast to cycle 1. This is also evident from visual observation, where a somewhat milky appearance is seen in cycle 2. Furthermore, an even larger reflection intensity is recovered after just a few seconds (see Figure 2) in cycle 2 when the voltage is removed, a time after which switching is already fully established[3] in cycle 1.

Corresponding differences show up in the non-specularly scattered intensity. In the zero voltage plots of Figure 6 the fingerprint state shows little scattering in cycle 2 and even less in cycle 1. The Grandjean states show similarly shaped distributions with the maxima at $\phi = \pm 9°$. However, the absolute value of scattering is higher in cycle 2. With the high frequency voltage applied the two maxima at 9° disappear. However, the central peaks appear broadend, particularly for cycle 2 (Figure 7).

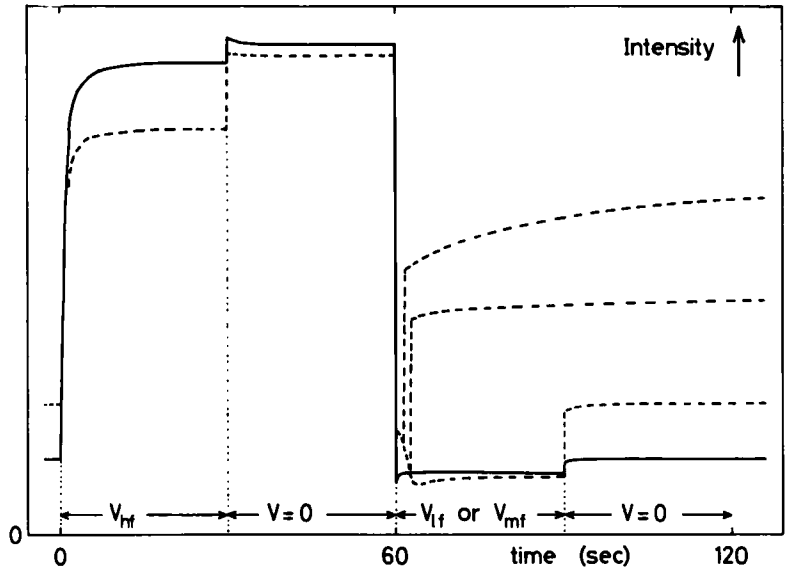

FIGURE 5 Intensity (arb. units) of specularly reflected light from a cholesteric layer as a function of time. The voltages corresponded to the cycle 1 (lines) and cycle 2 (dashed) as described in section 3.2. For cycle 2 two runs with a medium frequency applied for short times are also shown.

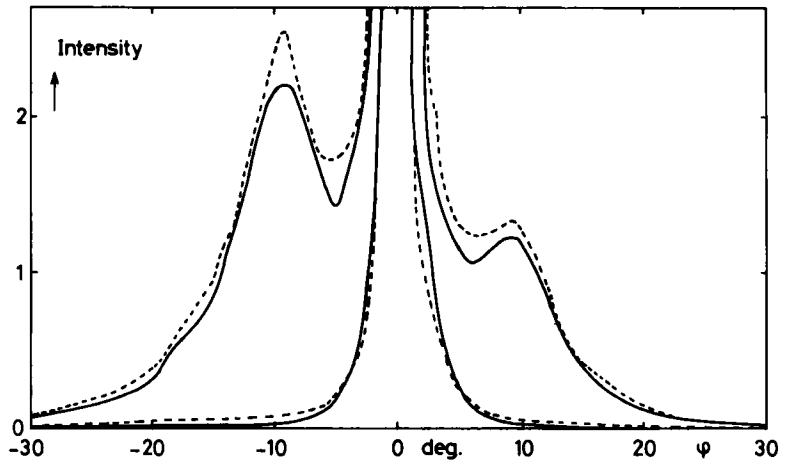

FIGURE 6 Smoothed curves of reflected intensity (arb. units) versus cell turning angle ϕ for the four stationary states of cycle 1 (lines) and 2 (dashed) after switching off the voltage.

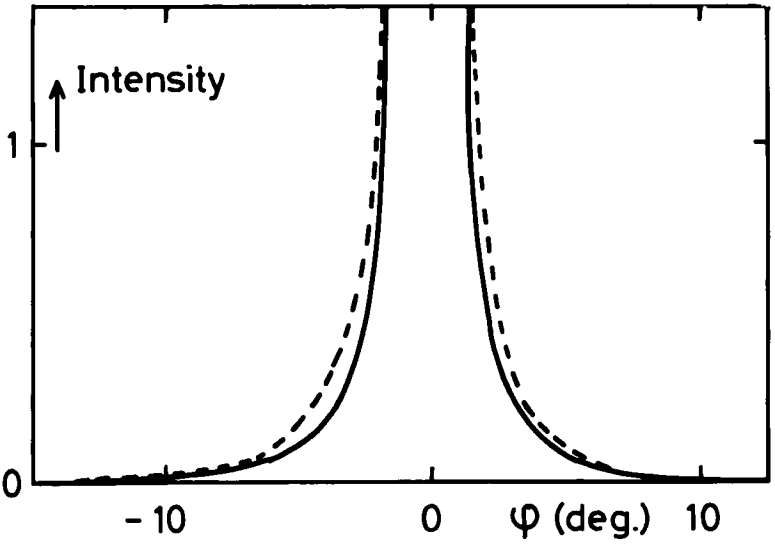

FIGURE 7 Smoothed curves of reflected intensity (arb. units) versus turning angle ϕ for the Grandjean states of cycle 1 (line) and 2 (dashed) with the voltage kept on. Sensitivity is reduced by a factor of 10 as compared to Figure 6.

All these findings indicate that for cycle 2 a richer net of disclinations develops than in cycle 1, this most certainly occurs during the dynamic scattering process. In addition, it appears that under continued application of the high frequency voltage, these nets can only relax to a finite extent which must be different for the two cycles. It appears that certain arrangements of disclinations remain frozen even in an applied high frequency voltage. It must be stressed, however, that the situation may be quite different for other types of substrate treatments.

In conclusion the dynamic scattering and the electrostatic reorientation processes lead to quite distinct textures. Whereas the Grandjean states are of comparable usefulness for display applications the fingerprint pattern shows considerably more reflection in the dynamic scattering case where its generation also requires much longer application of the switching voltage.

3.5 Influence of switching times on the reflection properties of the Grandjean state of cycle 1

For possible applications in a texture-change display it is of importance to know the light-reflecting properties of the Grandjean state

for various switching times. Starting from a fingerprint state generated by several applications of cycle 1 we have applied a 60 V_{rms} high-frequency signal for various time durations. In each case the reflected light was then measured as a function of the cell-rotation angle ϕ (see section 3.1). The results are shown in Figure 8. For short switching times a relatively broad distribution develops which shows no pronounced maxima and has a low intensity. For longer switching times, the distribution narrows, becomes more intensive and develops the pronounced peaks at $\phi \approx \pm 9°$. To make this more quantitative, we have plotted, in Figure 9, the switching-time dependence of a few characteristics quantities, namely the intensity of the specularly reflected light in the central peak, the integrated intensity of the scattered light and the first moment of $|\phi|$ which characterizes the width of the cone in which the diffuse scattering mainly takes place. These two latter quantities were calculated on the assumption that the average of reflected light for ϕ and $-\phi$, as shown in Figure 8, is representative for the average of the whole cone shell of light scattered at an angle ϕ off the specular direction.

For switching times of fractions of a second the specular and scattered intensities grow in proportion to each other and are of about the same magnitude. In this range the first moment of the distribution has its maximum value of about 16 degrees. For times above one second the specular intensity still grows at the expense of the diffuse intensity. The narrowing of the distribution is manifest in the decrease of the first moment below 13 degrees.

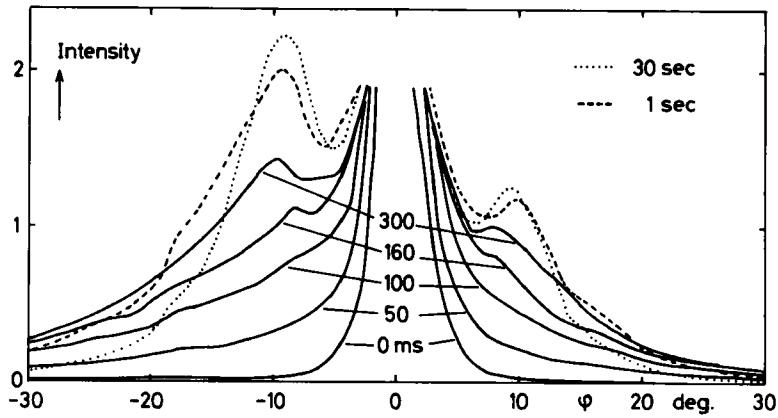

FIGURE 8 Distributions of reflected light (arb. units) versus cell turning angle ϕ for Grandjean states generated by cycle 1 by applying high frequency signals of various duration of the fingerprint state.

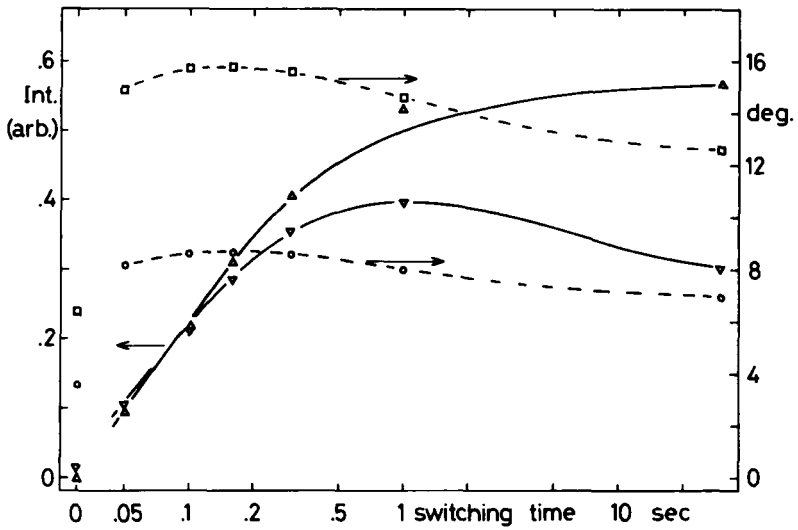

FIGURE 9 Switching time dependence of central-peak intensity (△) and integrated non specular intensity (▽) of the distributions shown in Figure 8. Also shown is the first moment of the cell rotation angle (□) as well as the first moment of helical-axis tilt angles as calculated by (Eq. 3.2) (○). The intensity is given in arbitrary units.

For the appearance of a reflective display a large portion of diffusely reflected light is advantageous because illumination at specular angles should be avoided because of reflections from the substrate surfaces. These lead to a brighter appearance of the fingerprint state and, hence, to reduced contrast. For this reason switching times should be chosen below 0.5 seconds.

By means of equation (3.2) the angular dependences of Figure 8 may be translated into a distribution of helix-axis angles if one trusts the picture of cholesteric domains. Correspondingly, Figure 9 also contains the switching time dependence of the first moment of the helix-axis tilt angles (again under the assumption of conical symmetry). It shows a decrease from nine to seven degrees with increasing switching times.

It is not hard to imagine that helix-angle distributions calculated from the measured scattered light distributions also show pronounced maxima which for the stationary case are at tilt angles of 6 degrees (after 30 sec. switching time). This indicates that quite well defined disclination patterns and domain tilts may prevail in the stationary state.

4. DISPLAY PARAMETERS

Detailed investigations on driving conditions of the two-frequency addressed cholesteric texture-change display are given elsewhere.[3,8] We present here a few of the most important points.

(i) Director alignment conditions are not very critical. Without special treatment one obtains a somewhat patchy appearance, while rubbed polyvinylalcohol layers tend to give a high specular reflection. Good results are found with oblique SiO evaporation.

(ii) The cell spacing is chosen to be low for fast switching speeds but for values below 10 **p** the reflection in the Grandjean state becomes reduced.

(iii) Switching voltages are bounded by the threshold for the cholesteric-nematic transition,[9]

$$V_{Ch,n} = \frac{d}{\mathbf{p}} \pi^2 (k_{22}/(\epsilon_0 \Delta\epsilon))^{1/2} \tag{4.1}$$

while switching times scale with the square of the applied field.[10] The values of high and low frequencies may be derived from the temperature dependence of f_c (Figure 2) and are typically 10 and 0.1 kHz.

(iv) Multiplexed operation[3,8] requires alternating high and low frequency voltages of duration τ_h and τ_ℓ. While the columns receive an amplitude of V_o, the addressed row has 2 V_o applied and the others zero voltage. To establish switching several (m) sequences of duration $\tau_h + \tau_\ell$ are needed before proceeding to the next row. The low frequency is most naturally chosen as $2/\tau_\ell$.

For our experimental displays the parameters are

$$\tau_h/\tau_\ell = 1 \pm 0.2$$

$$\tau_h + \tau_\ell = 10 - 20 \text{ ms}$$

$$f_h = 15 \text{ kHz}$$

$$m = 20 - 30$$

$$V_o = 20 \text{ Volts}$$

for the 13% w/w mixture described in Section 2. The display spacing is 10 μm for reasons of fabrication.

Acknowledgment

The author thanks A. Villiger for synthesizing molecule (I) and V. Kannookadan for the construction of displays.

References

1. P. G. de Gennes, *The Physics of Liquid Crystals*, (Clarendon Press, Oxford, 1974).
2. W. Haas, J. Adams and J. B. Flannery, *Phys. Rev. Lett.*, **24**, 577 (1970).
3. P. R. Gerber, *Appl. Phys. Lett.*, **44**, 932 (1984).
4. W. H. de Jeu, C. J. Gerritsma, P. van Zanten and W. J. A. Gossens, *Phys. Lett.*, **39A**, 355 (1972).
5. M. Schadt, *Mol. Cryst. Liq. Cryst.*, **89**, 77 (1982) and *Proc. 'Japan Display 83,'* 220 (1983).
6. W. Helfrich, *Mol. Cryst. Liq. Cryst.*, **21**, 187 (1973).
7. See *Jap. Pat.* 8346040, CA **99**, 158024q (1983).
8. P. R. Gerber, *to be published at Eurodisplay 84*, Paris, 1984.
9. P. G. de Gennes, *Solid State Comm.*, **6**, 163 (1968).
10. E. Jakeman and E. P. Raynes, *Phys. Lett.*, **39A**, 69 (1972).